Pure & Appl. Chem., Vol. 62, No. 11, pp. 2097–2106, 1990.
Printed in Great Britain.

Thermodynamics and structure in non-electrolyte solutions

L. Andreoli-Ball[1], S.J. Sun[1], L.M. Trejo[2], M. Costas[2], and D. Patterson*[1]

[1]. Chemistry Dept., McGill University, 801 Sherbrooke St., W., Montreal, PQ, Canada H3A 2K6

[2]. Facultad de Química, Universidad Nacional Autónoma de México, México D.F. 04510 México

Abstract - Thermodynamic quantities, particularly second-order are indicators of structure both in the pure components and in solution. Three solution structures are treated: (1) Non-randomness or concentration fluctuations due to "antipathy" between the components. This gives rise to a W-shape concentration dependence of the excess heat capacity C_p^E. Systems containing polyethers and alkanes illustrate the effect of molecular size on the W-shape C_p^E and its relation with a quantitative measure of non-randomness calculated from group-solution models, the concentration-concentration correlation function, S_{cc}. (2) Complexation between alcohol solute OH groups and proton-acceptor (PA), groups e.g. ketone or ester, in PA solvents or PA- inert solvent mixtures. The apparent molar heat capacity of the alcohol at infinite dilution changes with PA group concentration giving the ΔH and equilibrium constant for the complex. (3) Another "structure" is thought to arise when a highly flexible molecule, e.g. octamethylcyclotetrasiloxane comes into contact with small solvent molecules, e.g. benzene or dioxane. Thermodynamic excess quantities, supported by spectroscopy, suggest that these small molecules can intercalate between methyl groups of the dimethylsiloxane chain increasing the frequency of low-frequency high-amplitude modes of the flexible molecule. This in turn decreases free volume and affects a range of excess quantities.

INTRODUCTION

Thermodynamic results can lead to an intuitively satisfying picture of the interaction between components in solution. In particular, second-order quantities, e.g. heat capacity, are sensitive to the presence of "structure" or non-randomness which exists in the pure liquid components or are formed on mixing. In the present instance, we will deal with three such structures all in the solution, together with their effects on excess quantities, mainly C_p^E, or the apparent molar quantity of the solute, φ_c. The structures are: (1) non-randomness, i.e. "islands" in the solution caused by antipathy between the two components, bringing about a characteristic W-shape concentration dependence of C_p^E, negative towards the edges of the concentration range and positive toward the middle; (2) a hydrogen-bonded complex between an alcohol solute at high dilution and an "active" proton-acceptor solvent leading to an effect on φ_c of the solute, and (3), more speculatively, an insertion of a small solvent molecule between the methyl groups of a large and very flexible silicone solute raising the frequency of the silicone vibrations and, in consequence, lowering the surrounding free volume, thus affecting the thermodynamics of the mixture.

1. SOLUTION NON-RANDOMNESS AND THE W-SHAPE C_P^E

Thermodynamically, structure corresponds to a cohesion which lowers the enthalpy of a liquid, but which decreases in strength as the temperature increases, so that $dH/dT = C_p$ is enhanced. Heat capacity measurements are usually expressed in terms of the excess heat capacity of the system, defined as

$$C_p^E = C_p - x_1 C_{p,1}^o - x_2 C_{p,2}^o \qquad (1)$$

where the x_i are the mole fractions of the components and $C_{p,i}^o$ the heat capacities in the pure state. C_p^E represents the deviation from the ideal solution behavior which is given by $C_p^E = 0$. For mixtures where no special interactions take place, e.g. for mixtures of two short n-alkanes, C_p^E is negative but small, ca. 1 J/K mol, and can be explained as due to the change in free volume on mixing. Larger negative C_p^E are found if there is destruction on mixing of structure in one or both of the pure components. This is the case of long-chain n-alkanes mixed with globular molecules such as cyclohexane or benzene (ref. 1) where correlations of molecular orientations (CMO) in the pure n-alkanes are destroyed. Destruction of dipolar order in either or both components should also give $C_p^E < 0$. On the other hand, positive C_p^E has been associated with the formation of structure or organization in the solution, e.g. when an alcohol is dispersed in a hydrocarbon (ref. 2) or in mixtures where there is complex formation between the components (ref. 3). In these systems, the structure is given by the formation of different hydrogen-bonded species in the solution. In all of the above cases C_p^E curves are nearly

parabolic, i.e.. the maximum or minimum is located roughly at equimolar concentration. To these two types of concentration dependence Benson (ref. 4) and Grolier (ref. 5) and their collaborators added a quite intriguing dependence called a "W-shape" C_p^E characterized by the presence of two minima separated by a maximum or two concentration regions with positive curvature and one with negative curvature. Grolier and collaborators (ref. 6) have now found the W-shape C_p^E in a large number of systems many of which are referenced in ref. 6.

All of these systems have large values of H^E and G^E. Ref. 7 suggested that the W-shape could be understood in terms of another "structure" in solution which would produce $C_p^E > 0$, i.e. non-randomness or concentration fluctuations caused by the usual antipathy between components of a non-electrolyte mixture which ultimately, at low temperature, is responsible for the Upper Critical Solution Temperature (UCST). It is intuitively evident that solution non-randomness falls off towards the ends of the concentration range where dispersing one component at high dilution in the other must become random. Hence, the positive C_p^E will have a special shape as shown schematically in Fig. 1. Any model which incorporates non-randomness will give this qualitative result, e.g. the Guggenheim quasi-chemical approximation used in ref. 7. To the positive C_p^E must be added a negative contribution of parabolic shape due to destruction of dipolar order or correlations of molecular orientations in the pure components, or due to changes in free volume leading to the W-shape shown in Fig. 1.

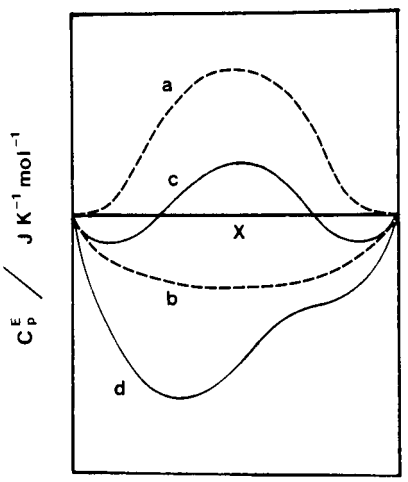

Fig. 1 Schematic of C_p^E against mole fraction. (a) positive contribution due to formation of structure, i.e. non-randomness, in solution, where molecular sizes of two components are similar, (b) negative "random" contribution due to destruction of CMO or dipolar order in pure components, (c) total W-shape C_p^E, (d) total W-shape C_p^E where non-randomness is less and there is a difference of component molecular sizes.

Rubio (ref. 8) at the Universidad Complutense, Madrid has proposed that a convenient measure of non-randomness is furnished by the concentration-concentration correlation function, S_{cc} which corresponds to the concentration fluctuations in the solution, given by the curvature of the solution free energy against concentration

$$S_{cc} = N\overline{\Delta x^2} = \left[\frac{\partial^2 G/RT}{\partial x^2}\right]^{-1} \tag{2}$$

If indeed both S_{cc} and the W-shape C_p^E are manifestations of non-randomness, then there should be a correlation between the two. The S_{cc} quantity may be obtained directly from light scattering, being given by the ratio of the experimental concentration fluctuation contribution to the Rayleigh ratio over its ideal, calculated value:

$$S_{cc} = x_1 x_2 \frac{R_c}{R_{c,ideal}} \tag{3}$$

Nevertheless, it can also be obtained approximately using group solution methods to give G of the solution. In terms of the simple Kehiaian-Grolier-Benson model (ref. 9) which uses a Flory-Huggins combinatorial term combined with interactions between molecular surfaces, we have:

$$S_{cc}^{-1} = (x_1 x_2)^{-1} + \left[\frac{r_1 - r_2}{x_1 r_1 + x_2 r_2}\right]^2 - \frac{2 q_1^2 q_2^2 (g_{12}/RT)}{(x_1 q_1 + x_2 q_2)^3} \tag{4}$$

IDEAL — NON–IDEAL COMBINATORIAL — INTERACTION

Here the first term, the ideal combinatorial, would give a maximum of the S_{cc} non-randomness parameter of only 0.25. The second, non-ideal combinatorial term depends on the numbers of segments, r_i, in the components defined in ref. 9 in terms of the molar volume of the methane molecule:

$$r_i = V_i / V_{CH_4} \tag{5}$$

The second term is positive and therefore decreases S_{cc} and non-randomness still further. However, the third, or interactional term, also non-ideal, and due to molecular antipathy is negative and therefore increases non-randomness and S_{cc}. The q parameters are surface areas of the molecules normalized by the surface of the methane molecule. g_{12} the average interactional free energy (antipathy) between segments of the components corresponds to w_{12} of regular solution theory or X_{12} of the Prigogine-Flory theory. The temperature dependence of this term is given by h_{12}, the average interactional enthalpy, which will be positive so that S_{cc} increases as T is lowered.

The first observation concerning eq. (4) is that if the interactional term becomes large enough through lowering T, then S_{cc}^{-1} ultimately falls to zero, $S_{cc} \longrightarrow \infty$ and the UCST is attained. One can expect that the W-shape C_p^E should be dramatically enhanced as the UCST is approached, and this has been confirmed for a number of systems (ref. 10). The second point is that the denominator of the interactional term is smallest for a small concentration of the component with large q. Hence, the maximum of S_{cc} will occur at a small concentration of the larger component. If q is replaced by r, i.e. holding to the simple Flory-Huggins theory the critical concentration where $S_{cc} \longrightarrow \infty$, lies at

$$(x_2/x_1)_c = (r_1/r_2)^{3/2} \tag{6}$$

showing the same displacement toward small concentration of the large component. Lastly, through most of the concentration range and, in particular, where it attains its maximum, the third term, and hence S_{cc} and non-randomness are increased by increasing the molecular sizes, i.e. either q_1 or q_2. If the non-randomness origin of the W-shape is correct, it should show corresponding effects of molecular size.

The oxaalkane (glyme) alkane set of systems is particularly convenient for a test of the correspondence between S_{cc} and the W-shape C_p^E. The glymes used were CH_3-O-$(CH_2$-O$)_n$-CH_3 represented by G_n with n = 1 to 4, i.e. monoglyme to tetraglyme, while a range of alkanes C_n were used with n running from 6 (hexane) to 30 for the lightly-branched (2,6,10,16,20,24-hexamethyltetracosane or squalane molecule. In fact, the work of ref. 4 was already made on the diglyme-heptane system and more extensive work by Benson and collaborators (ref. 11) with the W-shape C_p^E was on the triglyme - dodecane system. The q and r parameters are related to group contributions in ref 9. g_{12} reflects the O-CH_2 or O-CH_3 interactions which are taken to be equal and fitted to give $S_{cc} \longrightarrow \infty$ at 20.8° measured as the UCST for the tetraglyme-n-C_{10} system. The S_{cc} values calculated from eq. (4) are shown in Fig. 2 for the glyme-alkane systems at 25°. On the left, S_{cc} for $G_4 + C_6$ is small and the peak occurs at low glyme concentration reflecting the large molecular size of this glyme. Increasing n of the alkane series from 6 to 10 with the same glyme, increases S_{cc} as expected and shifts the maximum to higher glyme concentration consistent with the decreasing relative size of the tetraglyme. Turning to Fig. 3 we see the corresponding W-shape C_p^E curves which show high positive maxima between negative minima. The positive maxima clearly correspond in height and in concentration to the S_{cc} curves of Fig. 2 and must be due to solution non-randomness. The negative parts of the curves are almost overwhelmed by the central peaks. Nevertheless, they are significant and may be considered to be due to destruction of the n-alkane orientational order and dipolar order in the glyme and perhaps also glyme orientational order. (The light-scattering work by Flory (ref. 12) on glymes appears to show the enhancement of depolarized Raleigh scattering which Bothorel (ref. 13) used to prove the presence of CMO in long-chain n-alkane liquids.) Fig. 2 also shows S_{cc} for the triglyme-alkane set of systems starting with $G_3 + C_{10}$. The decrease of glyme molecular size from the $G_4 + C_{10}$ system has dramatically lowered the maximum and shifted it to higher glyme concentration. Building up the alkane size to $G_3 + C_{14}$ raises the maximum and further shifts it to higher glyme concentration. This evolution is followed in Fig. 4 by the W-shape values for the systems. Finally, Fig. 2 shows the S_{cc} values for G_2 starting with $G_2 + C_{16}$. The decrease of glyme molecular size from the $G_3 + C_{14}$ system has again decreased the maximum and shifted it to higher glyme concentration. Again, increasing alkane size from C_{16} to C_{30} enhances S_{cc} and in fact $S_{cc} \longrightarrow \infty$, the UCST for the $G_2 + C_{30}$ system being predicted at 25°. Fig 5. shows the corresponding C_p^E values for $G_2 + C_7$ (results of Benson and collaborators) for $G_2 + C_{16}$, $G_2 + C_{19}$ (2,6,10,14-tetramethylpentadecane or pristane) and $G_2 + C_{30}$ (squalane). Again the W-shape is predicted semi-quantitatively by the S_{cc} treatment, although C_p^E does not in fact go to infinity for squalane which would occur at the experimentally observed UCST at 20°. The magnitudes of the negative parts of the curves are difficult to interpret but probably reflect the CMO effect which is large for hexadecane, but small for the short heptane and for the branched alkanes pristane and squalane. Finally, Fig. 6 shows that there is an excellent correlation between the experimental concentration at which C_p^E attains its maximum and the concentration of the maximum in the theoretical S_{cc}. The conclusion is that the W-shape is undoubtedly due to solution non-randomness. Other work (ref. 14) shows that the W-shape becomes apparent ~ 100 K from the UCST which is a surprisingly large temperature interval. The visibility of the non-randomness "structure" in C_p^E seems to be due to the small size of the "normal" random solution C_p^E and the fact that the non-randomness and normal contributions to C_p^E are of different concentration dependence and of opposite sign. The two contributions should be of the same sign approaching the LCST in aqueous systems and hence, the W-shape should not be found. However, it should again be found in those systems where the LCST is due to a large difference in free volume (ref. 15) between the two components and where measurements would, unfortunately, be extremely difficult at the high temperatures required. Previous work (ref. 1) has shown that the other excess second-order quantities, e.g. dV^E/dT and $-dV^E/dP$ are also indicators of structure and these quantities should tend to infinity at the UCST. Nevertheless, both random and non-random contributions to dV^E/dT should usually be of positive sign and hence the W-shape would not appear. The W-shape should, however, occur for $-dV^E/dP$ in many systems but only at temperatures very close to the UCST. Thus, C_p^E within 100 K of the UCST seems to provide the best opportunity for observing this unusual concentration dependence.

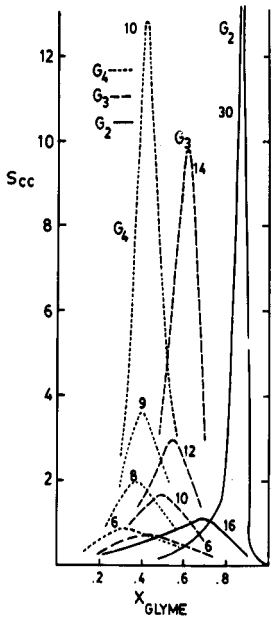

Fig. 2 The non-randomness function S_{cc} calculated at 25° from eq. (4) for tetraglyme (G_4),triglyme (G_3) and diglyme (G_2) mixed with alkanes (carbon numbers indicated), and plotted against glyme mole fraction.

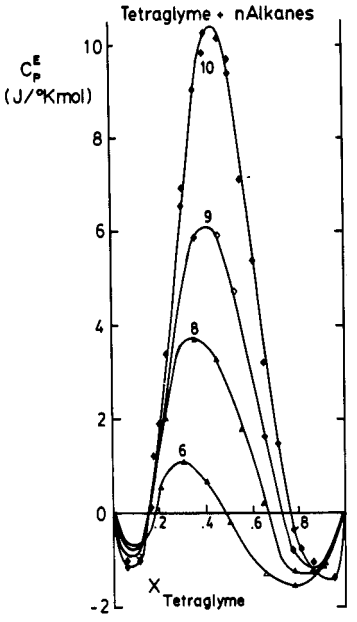

Fig. 3. C_p^E at 25° for tetraglyme, 2,5,8,11,14-pentaoxapentadecane + normal alkanes (carbon numbers indicated).

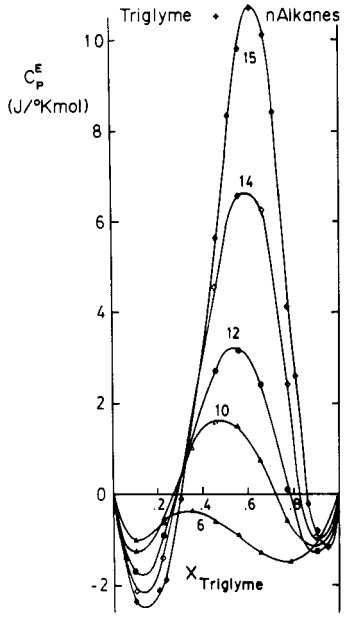

Fig. 4 C_p^E at 25° for triglyme, 2,5,8,11-tetraoxa dodecane + normal alkanes (carbon numbers indicated).

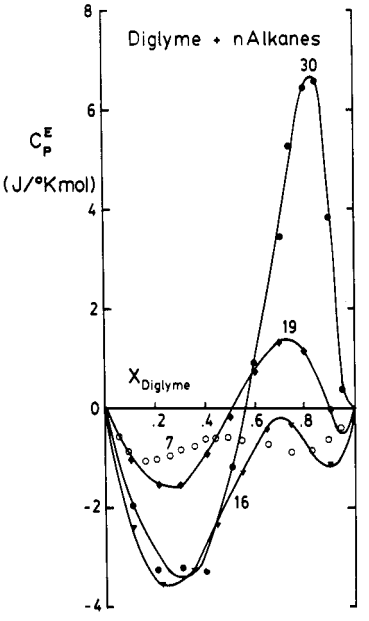

Fig. 5 C_p^E at 25° for diglyme, 2,5,8-trioxanonane + alkanes (carbon numbers indicated. Diglyme + n-heptane results from ref. 4. C_{19} = 2,6,10,14-tetramethyl-pentadecane (pristane); C_{30} = 2,6,10,15,19,23-hexamethyltetracosane (squalane).

Undoubtedly, the relation between S_{cc} and the W-shape is made most evident through studying mixtures where each component is drawn from a homologous series such as the $G_n + C_n$ set of systems. Some work has been done along those lines, e.g. with tetraoxasilanes + alkanes (ref. 16) and glymes + silicones and treated similarly to the $G_n + C_n$ systems, i.e. fitting the interactional free energy parameter to a known UCST. The results are that

the calculated S_{cc} predict the concentration at which the C_p^E peak occurs, but the heights of the C_p^E are not satisfactorily predicted. The trouble seems to be using a mean field theory like that of ref. 9 which must be incorrect approaching the UCST. Unfortunately, it is a difficult task for theory to move from the critical region near the UCST to the mean-field region far removed from that temperature.

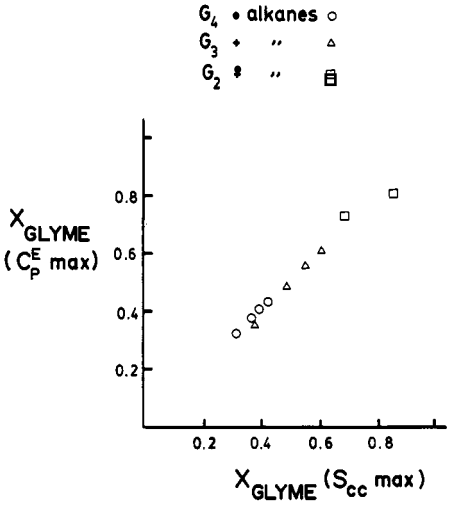

Fig. 6 Correlation between mole fractions of maxima of experimental W-shape C_p^E with mole fractions of maxima of calculated S_{cc} functions.

2. HEAT CAPACITY AND COMPLEX FORMATION IN SOLUTION

Self-association of alcohols in inert solvents can be studied to advantage using heat capacity either as the excess quantity of the mixture C_p^E or as φ_c, the apparent molar quantity of the alcohol as solute. Fig. 7 shows φ_c for hexanol in the inert solvent, dodecane (curve a). At infinite dilution φ_c starts from a low value, lim φ_c ($x \rightarrow 0$, inert) $\simeq$ 200 J K^{-1} mol^{-1} which corresponds to the heat capacity of the unassociated alcohol molecules, i.e. C_p due to vibrations within the molecule plus the "physical" interaction with the solvent. With increase of alcohol concentration, φ_c rises sharply above lim φ_c indicating formation of a micelle-like structure arising from alcohol self-association, mainly as tetramers (ref. 2) presumably cyclic in nature. A high maximum in $\varphi_c \simeq$ 500 J K^{-1} mol^{-1} is rapidly attained near 1 wt % alcohol followed by a slow decline, ultimately reaching C_p^δ of the pure alcohol (not shown). This last value still lies above lim φ_c because of the self-association in the pure liquid. However, the high maximum in φ_c indicates that, in some sense, there is much more structure at 1% concentration than in the pure alcohol liquid in spite of the higher degree of H-bonding in the pure liquid. At the lower concentration, an ideal random dispersal of alcohol molecules in the inert solvent would be over relatively large distances. Hence, the drawing-together of alcohol molecules into tetramers in the real solution constitutes a high degree of departure from randomness, or the creation of structure. On the other hand, at high alcohol concentration where random dispersal is over only small distances, the departure from randomness to bring about association is much less and hence "structure" and C_p are smaller. Another thermodynamic consequence is that at very low alcohol concentration where the alcohol in solution is largely unassociated S^E is positive due to the break-up of association in the pure liquid. However, S^E is negative throughout the rest of the concentration range reflecting the greater structure in the solution than in the pure liquid (ref. 17).

The associated part of φ_c is obtained by subtracting the limit of φ_c at infinite dilution in the inert solvent, i.e.

$$\varphi_c \text{ (assoc)} = \varphi_c - \lim \varphi_c \ (x \rightarrow 0, \text{ inert}) \tag{7}$$

φ_c (assoc) has now been obtained (ref. 2) for various 1-alkanol-alkane systems giving a variety of curves as a function of concentration with maxima occurring at different alcohol weight fractions. However, a more fundamental concentration variable has been advanced (ref. 18), i.e. a concentration of OH groups in the solution,

$$\psi_1 = \text{no OH groups/total groups in solution}$$

$$= x_1/(x_1 r_A + x_2 r_2) \tag{8}$$

with r_A and r_2 being the numbers of segments in the alcohol and inert solvent, respectively, as defined in ref. 18 or 2. When plotted against ψ_1 all points for the different 1-alkanol-inert systems fall on a single corresponding states curve (CSC) with small deviations for methanol and ethanol systems (ref. 2b). The CSC curve may be reproduced through simple association models, e.g. Treszczanowicz-Kehiaian (TK) (ref. 19). Also see models used by Stokes et al (ref. 20) and more recently by Kohler and associates (ref. 21). The shape of the CSC curve

gives the number of alcohol molecules (four) in the multimers forming in solution, while the height of the maximum and the concentration at which it occurs give, respectively, ΔH and the equilibrium constant K_4 for OH-OH H-bonding in the tetramers. The fact that almost all 1-alkanol-inert systems follow a single CSC shows that ΔH and K_4 are the same for 1-alkanols independent of chain length. However, alcohols where steric hindrance impedes H-bonding (ref. 22) show different ΔH and K_4 values and also give evidence of other multimers. In particular, phenols with sterically hindering groups in the 2 and 6 positions are marked by an almost complete absence of self-association (ref. 23).

C_p is also valuable when the inert solvent is replaced by an "active" solvent containing proton-acceptor (PA) groups with which the alcohol OH's can complex, e.g. ester or ketone groups. The "active" solvent may be either a pure PA liquid, or a mixture of PA molecules with an inert solvent (ref. 24). Two competing structures now occur: tetramers caused by OH-OH bonding (A_4) and complexes (AB) from OH-PA group bonding. The association theory indicates that no difference exists between using a single PA solvent or the PA-inert mixture. In either case, the important variable is the concentration of PA groups either in the PA molecules of the single PA liquid or in the PA-inert mixture. This concentration is

$$\Psi_2 = \frac{x_2}{x_2 r_2 + x_3 r_3} \tag{9}$$

where x_2, x_3 and r_2 and r_3 are now the mole fractions and number of segments in PA and inert molecules.

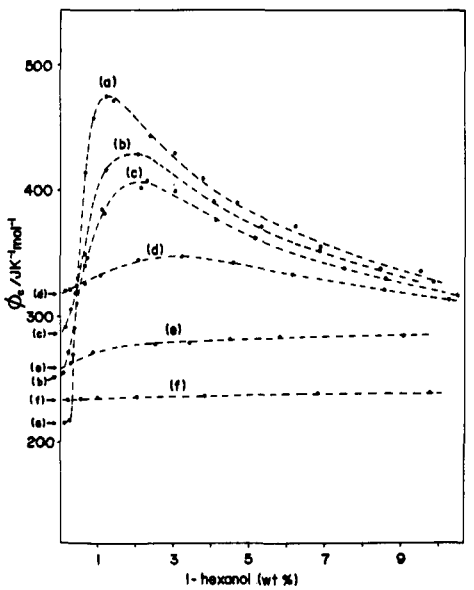

Fig. 7 Apparent molar heat capacity, φ_c, at 25° for 1-hexanol in n-dodecane, (a) and for 1-hexanol in n-dodecane solutions of methyl acetate [(b) 2.0, (c) 43, (d) 10.2 and (e) 30.0 wt %] and 1-hexanol in methyl acetate (f).

Fig. 7 shows φ_c of hexanol as a function of its wt % in mixtures of the PA methyl acetate with dodecane at increasing wt % and finally of hexanol in pure methyl acetate. Complexation competes with self-association so that in the 1% hexanol region, as the methyl acetate concentration is increased in the solvent mixture, the maximum in φ_c decreases continuously and is displaced to higher hexanol concentration until for the alcohol in pure methyl acetate the maximum has disappeared. Identical behaviour has been found for hexanol in 2-pentanone + n-C_{12} mixtures. On the other hand, at very low concentration of alcohol or at infinite dilution where self-association has been eliminated, lim φ_c ($x \rightarrow 0$) first increases with increasing PA concentration then passes through a maximum and decreases again. The associational part of this limit in an active solvent, lim φ_c (assoc) is obtained from eq. (7) and will also pass through a maximum.

The behaviour of the associational part of the limit is seen more clearly in Fig. 8 where it is plotted against log φ_2 for two sets of systems: hexanol-(2-pentanone + n-C_{12}) and hexanol- (methyl acetate + n-C_{12}). The increase and decrease with increasing PA group concentration is clearly seen in the characteristic bell-shaped curves and is analogous to the behaviour of φ_c of an alcohol in an inert solvent which also passes through a maximum for increasing alcohol concentration. At very low PA concentration, PA groups surrounding an alcohol molecule are too dilute for complexes to be formed and lim φ_c (assoc) is small. A higher concentration of PA groups corresponding to the maximum allows complexation but requires a high degree of non-randomness, i.e. structure, to bring OH and PA groups together to form the complex and hence gives a high value of lim φ_c (assoc). A very high PA concentration constitutes less non-randomness, less structure and therefore smaller values of the limit.

The behaviour shown in Fig. 8 can be understood more quantitatively through the TK association model in which the energy of the alcohol molecule is plotted against T for two different alcohol concentrations, ~ 1 wt % (Fig. 9a) and secondly at very low concentration corresponding to infinite dilution (Fig. 9b). In both cases, three energy levels are available for an alcohol molecule (these have been fixed through fitting to experiment for self-association and complex formation.) The lowest level and strongest cohesion corresponds to the alcohol molecule in a tetramer complex, A_4. The intermediate level corresponds to the alcohol complexed to a PA

molecule (AB) and finally the highest energy level is reached by the free alcohol molecule dissociated from PA and other alcohol molecules. At lowest T, the alcohol molecule is found in the lowest energy state. Then with increase of temperature, for the alcohol-inert solvent case the alcohol energy increases directly from the A_4 level to A since no PA molecules are available for complexation in an intermediate energy state. However, with PA molecules present, as the temperature rises, the alcohol molecules first associate with PA molecules and then free themselves to dissociate completely. The concentration of PA groups affects the temperatures at which the A_4 change to AB and then the AB to A. The higher the PA concentration, the more attractive the AB state and the longer the temperature interval spent in that state.

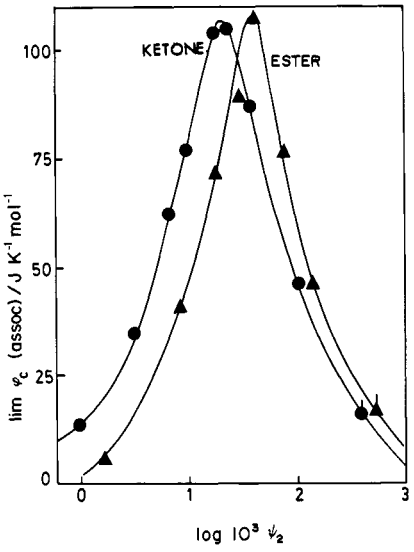

Fig. 8 The limit at infinite dilution of φ_c (assoc), defined by eq. (7), for 1-hexanol in 2-pentanone + dodecane mixtures (●) and in pure 2-pentanone (◆) and in methyl acetate + dodecane mixtures (▲) and in pure methyl acetate (▲) plotted against log proton-acceptor group concentration, ψ_2 defined by eq. (9).

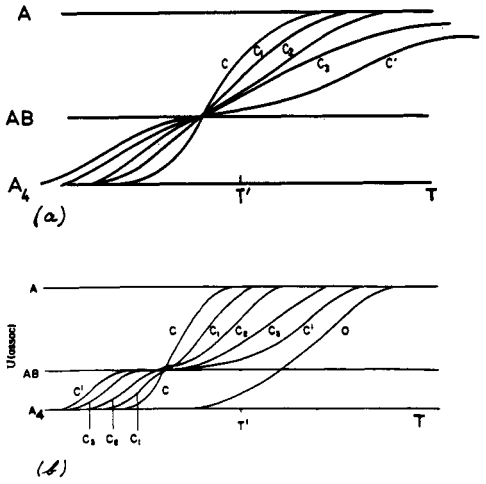

Fig. 9 Schematic of the energy against T for an inert alcohol in an inert solvent (C) in proton-acceptor (PA) + inert mixtures of increasing PA concentration (C_1, C_2, C_3) and in pure PA (C). (a) for alcohol at ~ 1 wt % showing $\varphi_c = dU/dT$ at experimental temperature T' continuously decreasing with increasing PA concentration, (b) for alcohol at lower concentration showing $\varphi_c = dU/dT$ at T passing through a maximum with increasing PA concentration.

The slope dU/dT gives the heat capacity φ_c. It is clear that in Fig. 9a for the 1% concentration and at the experimental temperature T', φ_c decreases continuously with increasing PA concentration in the PA-inert mixture. This is in harmony with the experimental findings of Fig. 7. The increasing stability of the AB complexes decreases the heat capacity effect at the temperature T'. However, at a lower concentration of alcohol corresponding to infinite dilution of alcohol in Fig. 9b, the curves have moved to lower temperature and it is seen that φ_c is low for small PA concentration, then increases and finally falls again. This corresponds to the maximum seen in Fig. 8.

The TK model gives a quantitative estimation both of the course of φ_c as a function of alcohol concentration in the PA environment and also for the way the lim φ_c (assoc) changes with the PA group concentration. The lim φ_c (assoc) for the general case of formation of AB_j complexes is found to be

$$\lim \varphi_c \text{ (assoc)}/R = j^2 \left[\frac{\Delta H_{11}}{RT}\right]^2 \left[(K_{11}\psi_2)^{j/2} + (K_{11}\psi_2)^{-j/2}\right]^{-2} \qquad (10)$$

where ΔH_{11} is the energy of complexation of the alcohol to the PA, K_{11} is the equilibrium constant and ψ_2 is the PA group concentration defined by eq. (9) for the PA- inert mixture. Eq. (10) shows that lim φ_c (assoc) against log ψ_2 will be a bell-like curve as in Fig. 7, symmetrical about the maximum which occurs for $\psi_2 = K_{11}^{-1}$ and the maximum value of lim φ_c (assoc) / R = $(j\Delta H_{11}/2RT)^2$. The data in Fig. 8 are similar for the OH-ketone and OH-ester interaction. They are both fitted best by a j number slightly greater than 1, i.e. 1.4, the meaning of which is difficult to ascertain. The equal maxima for the OH-ketone and OH-ester systems show that the OH for these interactions are similar. Nevertheless, the position of the maximum shows there is a larger equilibrium constant for the OH-ketone interaction by a factor of ~ 2. This is consistent with the β parameter for hydrogen-bond acceptor basicity which has a larger value (ref. 25) for ketones than for esters (0.50 for 2-pentanone and 0.42 for methyl acetate.) The curves in Fig. 8 represent CSC, i.e. data with ketone-inert and with ester-inert

mixtures should all fall on the two curves found there. Data using pure ketones and esters should also fall on the curves at high ψ_2 expressing the Bronsted Principle of Congruence. Preliminary results are promising.

3. EXTERNAL DEGREES OF FREEDOM IN DIMETHYLSILOXANE SOLUTIONS

The role of free volume and the equation of state was introduced into solution thermodynamics by the Prigogine-Flory (ref. 26) (PF) theory. Any thermodynamic property of a liquid, e.g. the molar volume V(T) is expressed as the product of two factors: (1) the "core" volume or reduction parameter V^* independent of T and equal to the molar volume at 0 K and (2) the reduced volume $\tilde{V}(T) > 1$, expressing free volume which "expands" V^* up to the molar volume at T. $\tilde{V}$ is a universal function of the reduced temperature T which measures the effectiveness of the thermal energy kT in expanding the liquid. It is a dimensionless ratio of two energies, $U_{external}$ promoting expansion and $U_{cohesive}$ restricting it:

$$\tilde{T} = \frac{U_{external}}{U_{cohesive}} = \frac{S^* T}{U^*} = \frac{c\, k\, T}{q\, \varepsilon^*} \tag{11}$$

Here q, as in the Kehiaian-Grolier-Benson theory, measures the surface area of the molecule and ε^* is the depth of the potential well for segmental interaction so that the denominator constitutes U^* the reduction parameter for energy. The numerator recognizes that all vibrations of the molecule do not affect the volume. Hence, 3c is the number of external, volume-dependent degrees of freedom/mole of liquid. These will include low-frequency modes which were translations and rotations in the gas phase and also similar modes corresponding to movements within the molecule itself. ck constitutes a characteristic entropy related to all of these frequencies which may perhaps be considered as equivalent to n classical oscillators of frequency υ. Then, expressed per mole,

$$S^* = cR = nR\,[\,1 + \ln(kT/h\nu)\,] \tag{12}$$

In passing to the solution, Prigogine (ref. 26) made the simple assumption that the external degrees of freedom were unaffected by the molecular interaction, which in hindsight seems difficult to justify in view of the external character of these degrees of freedom. Nevertheless, in the single-liquid approximation for the solution, the molar c is given by

$$c = x_1 c_1 + x_2 c_2\,;\; S^* = x_1 S_1^* + x_2 S_2^* \tag{13}$$

The other combining rules are also simple

$$V^* = x_1 V_1^* + x_2 V_2^*$$

$$U^* = x_1 U_1^* + x_2 U_2^* - x_1 V_1^* \theta_2 X_{12} \tag{14}$$

where θ_2 is the surface fraction of component 2. X_{12}, which corresponds to w_{12} and g_{12} above, is positive unless specific interactions occur between the components. It is usually fitted to the excess enthalpy H^E for the solution after which the other excess quantities can be calculated and compared with experiment.

The classical lattice theories like regular solution theory or the Flory-Huggins recognized only effects of X_{12} whereas the Prigogine-Flory theory emphasizes the role in solution thermodynamics of the free volume difference between the components. This is usually large whenever there is a large difference of molecular weights, typically in polymer solutions. In solutions dominated by this difference $\tilde{V}$ undergoes a net decrease during mixing. This results in a negative V^E and residual or non-combinatorial S^E and hence low solubility of the polymer and a large χ parameter. Furthermore, the second-order quantities C_p^E, dV^E/dT (excess expansibility) and $-dV^E/dP$ (essentially excess compressibility) will be negative.

On the other hand, the free volume difference is rather small for most mixtures where both components are small molecules whose thermodynamics is therefore usually dominated by X_{12}. However, X_{12} as well as having a direct effect in H^E as in the lattice theories plays a free volume role since it decreases U^* of the solution and increases T and the free volume $\tilde{V}$ in eq. (14) and (11). Thus its effect is to give increased free volume to the solution and increase expansibility and compressibility, i.e. H^E and V^E are positive as well as the second-order excess quantities C_p^E, dV^E/dT and $-dV^E/dP$.

In spite of the great success of the PF theory, systems containing polydimethylsiloxane (PDMS) or its low molecular weight analogues, the silicones, have proven the exception. PDMS is remarkable for its low cohesion and high flexibility which combine to give a value of α, the thermal expansion coefficient, more appropriate to a low molecular weight compound than a high polymer. It has a free volume approaching that of its solvents and consistent with this, the predicted volume of mixing for polymer solutions and the residual entropy are positive. The experimental values are however negative, i.e. the PF theory fails for this class of systems (ref. 27). We have made further tests of the PF theory using a range of volume-related excess quantities, V^E, dV^E/dT and $-dV^E/dP$ (ref. 28). The silicone chosen is octamethyltetrasiloxane (OMCTS), the cyclic tetramer of PDMS mixed

with solvents composed of very small molecules, benzene, cyclohexane, cyclopentane and dioxane. In spite of its extremely high molecular weight, 297, OMCTS and its solvents have very similar degrees of thermal expansion and hence these solutions are dominated by X_{12} effects rather those arising from free volume differences. Fig. 10 shows the PF predictions of V^E for several OMCTS systems. Consistent with the large positive values of H^E and corresponding values of X_{12}, V^E are predicted to be positive for these X_{12}-dominated systems. Yet the experimental quantities are either negative or very much smaller than predicted. Similar discrepancies are found for dV^E/dT and $-dV^E/dP$ which are predicted positive by the PF theory for OMCTS + benzene, cyclohexane and cyclopentane, whereas the experimental results are all negative (not shown here).

The discrepancy between theory and experiment in the case of PDMS solutions has stimulated speculation. Flory and Shih (ref. 27) have suggested that the origin may lie in an insertion of small solvent molecules such as benzene or CCl_4 between the methyl groups of the dimethylsiloxane backbone, i.e. a packing effect equivalent to the creation of "structure" in the solution. Consistent with such a hypothesis we find that the PF theory gives good predictions for V^E with X_{12} fitted to H^E when solvents of molecular size greater than benzene or cyclohexane are used. Shiomi et al (ref. 29) and Li et al (ref. 30) have relaxed the assumption of eq. (13) and have, amongst other possibilities, allowed

$$c = x_1 c_1 + x_2 c_2 + \Delta c \; ; \; \Delta c < 0$$

$$S^* = x_1 S_1^* + x_2 S_2^* + \Delta S^* \; ; \; \Delta S^* < 0 \qquad (15)$$

whence the predicted $\tilde{T}$ will be less than that calculated using eq. (13) bringing a reduction of V and the calculated V^E. In other words, the effect of X_{12} in increasing $\tilde{V}$ by lowering U^* is counter-balanced by reducing $U_{external}$ through the effect of Δc. The table for OMCTS + benzene shows the experimental results for equimolar composition, then the predictions using only X_{12} fitted to H^E, i.e. the usual application of the PF theory. Then come the predictions with X_{12} fitted to V^E where the volume-related excess quantities are well-predicted, but H^E turns out negative due to the almost zero value of X_{12} required to fit V^E. Next, X_{12} is fitted to H^E but the eq. (14) for V^* is changed to fit V^E, i.e. packing is assumed along the lines suggested by Flory and Shih which might be considered as decreasing V^* below the simple linearity expressed by eq. (14). Although H^E and V^E are well-predicted the second-order quantities dV^E/dT and $-dV^E/dP$ are not, forcing us to turn to fitting X_{12} to H^E and Δc to V^E. When this is done, fairly good results are found for all of the quantities, the fitting parameter being $\Delta S^*/S^*_{OMCTS} = 0.013$ for benzene.

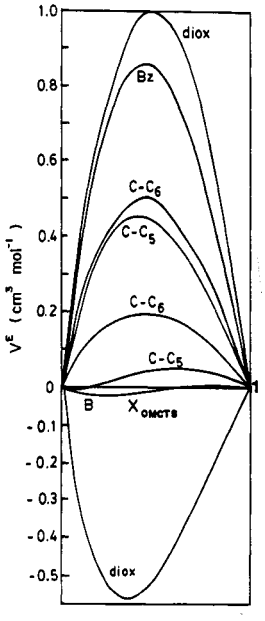

Fig. 10 Molar V^E for OMCTS + dioxane, benzene, cyclohexane and cyclopentane at 25°. In all cases, upper curve is experimental and lower is theoretical calculated by the Prigogine-Flory theory with X_{12} fitted to H^E.

Table 1. Equimolar Thermodynamic Data for OMCTS + benzene at 25°C

	H^E / J cm^{-3}mol	V^E / cm^3 mol	dV^E/dT / 10^{-3}cm^3 K mol	$-dV^E/dP$ / 10^{-4}cm^3 atm mol
experimental	793	-0.009	-0.22	-7.5
theor. X_{12} (H^E)	793	0.855	6.83	3.15
theor. X_{12} (V^E)	-67	-0.009	-0.08	-10.1
theor. X_{12} (H^E), V^* (V^E)	793	-0.009	5.76	3.0
theor. X_{12} (H^E), S^* (V^E)	793	-0.009	-0.1	-5.9

The next point is whether this relatively small change of S^*_{OMCTS} can be consistent with spectroscopic evidence. Raman spectroscopy was performed and in particular the 145 cm^{-1} out-of-plane ring deformation of OMCTS was observed to be displaced to higher frequency when the OMCTS was dispersed at 50% by weight in dioxane (by 5 cm^{-1}) and benzene (by 3 cm^{-1}). On the other hand, in diphenylmethane, a large-molecule solvent where V^E is well-predicted by the standard PF theory, we found no displacement of the 145 cm^{-1} band. Accepting the simple equation (12) for the characteristic entropy S^*, a change of 5 cm^{-1} in the frequency of the OMCTS molecule would lead to

$$\frac{\Delta S^*}{S^*} = -\frac{\Delta \nu}{\nu} \frac{x_{OMCTS}}{1 + \ln(kT/h\nu)} \tag{16}$$

with the result for $\Delta S^*/S^*_{OMCTS} = 0.013$ one calculates $\Delta \upsilon = 5$ cm^{-1} which is the right order of magnitude. Although the change of external degrees of freedom must be considered speculative we believe that it should be considered, and that excess second-order thermodynamic quantities are of interest in testing this hypothesis.

Acknowledgements

We thank the Natural Sciences Engineering Research Council of Canada, the Consejo Nacional de Ciencia y Tecnología de México and World University Service of Canada for a scholarship to L.M.T.

REFERENCES

1. S.N. Bhattacharyya and D. Patterson, J. Phys. Chem., 83, 2979 (1979); M. Costas, S.N. Bhattacharyya and D. Patterson, J. Chem. Soc. Faraday Trans. 1, 81, 387 (1985); G. Tardajos, E. Aicart, M. Costas and D. Patterson, J. Chem. Soc. Faraday Trans. 1, 82, 2977 (1986).
2. (a) M. Costas and D. Patterson, J. Chem. Soc. Faraday Trans., 81, 635 (1985), (b) L. Andreoli-Ball, D. Patterson, M. Costas and M. Caceres-Alonso, J. Chem. Soc. Faraday Trans. 1, 84, 3991 (1988).
3. M. Costas, Z. Yao, and D. Patterson, J. Chem. Soc. Faraday Trans. 1, 85, 2211 (1989).
4. F. Kimura, P.J. D'Arcy, M.E. Sugamori and G.C. Benson, Thermochimica Acta, 64, 149 (1983).
5. J.P.E. Grolier, A. Inglese and E. Wilhelm, J. Chem. Thermodyn. 16, 67 (1984); A. Inglese, E. Wilhelm and J.P.E. Grolier, 37th Annual Calorimetry Conf., Snowbird UT, 1982, paper 54.
6. M. Pintos, R. Bravo Baluja, M.I. Paz Andrade, G. Roux-Desgranges and J.P.E. Grolier, Can. J. Chem., 66, 1179 (1988) and refs. therein.
7. M.E. St. Victor and D. Patterson, Fluid Phase Equilibria, 37, 237 (1987).
8. R.G. Rubio, M. Caceres, R.M. Masegosa, L. Andreoli-Ball, M. Costas and D. Patterson, Ber. Bunsenges. Phys. Chem., 93, 48 (1989).
9. H.V. Kehiaian, J.P.E. Grolier and G.C. Benson, J. Chim. Phys., 75, 1031 (1975).
10. M.E. St. Victor and D. Patterson, Thermochimica Acta, 159, 177 (1990).
11. G.C. Benson, M.K. Kumaran, T. Treszczanowicz, P.J. D'Arcy and C.J. Halpin, Thermochimica Acta, 95, 59 (1985).
12. G.D. Patterson and P.J. Flory, J. Chem. Soc. Faraday Trans. 2, 68, 1111 (1972).
13. P. Bothorel, J. Colloid Sci., 27, 529 (1968). P. Tancrede, P. Bothorel, P. de St. Romain and D. Patterson, J. Chem. Soc., Faraday Trans. 2, 73, 15 (1977).
14. L. Andreoli-Ball, M. Costas, D. Patterson, R.G. Rubio, R.M. Masegosa and M. Caceres, Ber. Bunsenges. Phys. Chem. 93, 882 (1989).
15. M.E. St. Victor and D. Patterson, Thermochimica Acta, 149, 259 (1989).
16. L. Andreoli-Ball and D. Patterson, Can. J. Chem., July 1990.
17. J.S. Rowlinson and F.L. Swinton, Liquids and Liquid Mixtures 3rd ed., Butterworth's, London, p. 171 (1982).
18. J. Pouchly, J. Chem. Soc., Faraday Trans. 1, 82, 1609 (1986).
19. H. Kehiaian and A.J. Treszczanowicz, Bull. Soc. Chim. Fr, 5, 1561 (1969).
20. R.H. Stokes, J. Chem. Soc. Faraday Trans. 1, 73, 1140 (1977).
21. A. Liu, F. Kohler, L. Karrer, J. Gaube and P. Spellucci, Pure Appl. Chem., 61, 1441 (1989).
22. M. Caceres, M. Costas, L. Andreoli-Ball and D. Patterson, Can. J. Chem. 66, 989 (1988).
23. S. Perez-Casas and M. Costas, 4th International Symposium on Solubility Phenomena, Troy NY, 1990.
24. M. Costas, Z. Yao and D. Patterson, J. Chem. Soc. Faraday Trans. 1, 85, 2211 (1989).
25. M.J. Kamlett, J.L.M. Abboud, M.H. Abraham and R.W. Taft, J. Org. Chem. 48, 2877 (1983).
26. I. Prigogine (with the collaboration of V. Mathol and A. Bellemans), The Molecular Theory of Solutions, North-Holland, Amsterdam, ch. 16, 1975; P.J. Flory, Disc. Faraday Soc., 49, 7 (1970).
27. P.J. Flory and H. Shih, Macromolecules, 5, 761 (1972); R.S. Chahal, W.P. Kao and D. Patterson, J. Chem. Soc. Faraday Trans. 1, 69, 1849 (1972).
28. S.N. Bhattacharyya, M Costas, S.J. Sun and D. Patterson to be published.
29. T. Shiomi, K. Fujisawa, F. Hamada and A. Nakajima, J. Chem. Soc., Faraday Trans. 2, 76, 895 (1980).
30. P. Li, S. Krause and H.B. Hollinger, J. Polymer Sci., 1990 (in press).